Research article

LUMINESCENCE
The Journal of Biological and Chemical Luminescence

Received: 24 May 2009, Revised: 25 December 2009, Accepted: 21 January 2010, Published online in Wiley Online Library: 22 March 2010

(wileyonlinelibrary.com) DOI 10.1002/bio.1207

A novel method for sensing of methimazole using gold nanoparticle-catalyzed chemiluminescent reaction

Zonghai Sheng, Heyou Han* and Gaodong Yang

ABSTRACT: Based on the inhibition effect of methimazole (MMI) on the reaction of luminol–H_2O_2 catalyzed by gold nanoparticles, a novel chemiluminescence (CL) method was developed for the determination of MMI. Under the optimum conditions, the relative CL intensity was linearly related to MMI concentration in the range from 5.0×10^{-8} to 5.0×10^{-5} mol L^{-1}. The detection limit was 1.6×10^{-8} mol L^{-1} (S/N = 3), and the RSD for 6.0×10^{-6} mol L^{-1} MMI was 4.8% (n = 11). This method has high sensitivity, wide linear range, inexpensive instrumentation and has been applied to detect MMI in pharmaceutical tablets and pig serum samples. Furthermore, a possible reaction mechanism is discussed. Copyright © 2010 John Wiley & Sons, Ltd.

Keywords: chemiluminescence; luminol; gold nanoparticles; methimazole

Introduction

Chemiluminescence (CL) analysis is a simple, rapid, and sensitive analytical method (1–3). Some catalysts, such as metal ions, metal complex and enzymes, can be used to effectively catalyze the CL reaction (4–7). Recent research has shown that gold nanoparticles (NPs), one of the most widely used noble metal nanomaterials, could also participate in CL reactions as a catalyst (8–10). Moreover, the catalytic activity of gold NPs was 100 times greater than that of some metal ions under the same conditions (11). Therefore, gold NPs-enhanced CL has attracted much attention in recent years. For example, Lin's group reported first the behaviour of the bis(2,4,6-trichlorophyenyl) oxalate–H_2O_2–gold NPs CL system in the presence of different surfactants (12). Zhao *et al.* developed a gold NPs-enhanced capillary electrophoresis–CL assay of trace uric acid (13). Qi and coworkers reported a label-free and homogeneous DNA hybridization analytical method using a luminol–H_2O_2–gold NPs CL system (14). Wang's group described a flow injection CL method for the determination of fluoroquinolone derivative using gold NPs as a catalyst (15). However, the analytical application of the CL reaction catalyzed by gold NPs has been little reported in drug analysis (16–18).

Methimazole (2-mercapto-1-methylimidazole, MMI; Fig. 1) is an orally active drug used in the therapy of hyperthyreosis in humans and against Grave's disease (19). In addition, MMI has been applied illegally to cattle as a fattening agent, which leads to a reduction of the meat quality (20). The uncontrolled introduction of MMI into the human food chain could have serious health implications. Therefore, the detection of MMI in drugs is current important. At present, several analytical methods have been developed for the determination of MMI including capillary zone electrophoresis, liquid chromatography, gas chromatography–mass spectrometry, and so on (21–25). These methods have their respective shortcomings, such as being time-consuming and laborious and requiring complicated instrumentation. Recently, Economou and co-workers reported a CL method for the determination of MMI based on the inhibition of the luminol–H_2O_2 reaction catalyzed by Cu^{2+} (26). However, the poor selectivity and sensitivity limited the application of this method to a wider field.

In this paper, we found that the CL intensity of the reaction of luminol–H_2O_2 catalyzed by gold NPs was strongly decreased in the presence of MMI and the relative CL intensity was linearly related to the amount of MMI added. A novel gold NPs-catalyzed CL method for the sensitive determination of MMI in pharmaceutical tablet and pig serum sample was developed. A possible reaction mechanism was also discussed.

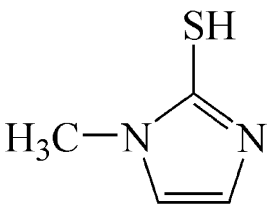

Figure 1. Chemical structure of methimazole.

Experimental

Reagents and chemicals

All the solutions were prepared using reagent-grade chemicals and Milli-Q water was used throughout. A 0.01 mol L^{-1} stock

* Correspondence to: Heyou Han, College of Science, the State Key Laboratory of Agricultural Microbiology, Huazhong Agricultural University, Wuhan, 430070, People's Republic of China. E-mail: hyhan@mail.hzau.edu.cn

College of Science, the State Key Laboratory of Agricultural Microbiology, Huazhong Agricultural University, Wuhan, 430070, People's Republic of China

LUMINESCENCE
The Journal of Biological and Chemical Luminescence

solution of luminol (Sigma, USA) was prepared in 0.1 mol L^{-1} sodium hydroxide solution without further purification. Working solution of luminol was prepared by diluting the stock solution with 0.01 mol L^{-1} NaOH solution. $HAuCl_4 \cdot 4H_2O$ was obtained from Sinopharm Chemical Reagent Co. Ltd. A 0.04 mol L^{-1} trisodium citrate solution was prepared by dissolving trisodium citrate (Sinopharm Chemical Reagent Co. Ltd) in water. MMI (Sigma, St Louis, MO, USA) was prepared by dissolving it in water and the standard solutions were obtained by diluting them to the wanted concentration with water. Ten MMI tablets (BeiJing TaiYang Pharmaceutical Industry Co. Ltd) were powdered and dissolved in 20 mL water. The solution was centrifuged and filtered through a Micron separation Inc. 0.22 µm nylon filter. The pig serum samples were obtained from the State Key Laboratory of Agricultural Microbiology (Huazhong Agricultural University). Before detection, the pig serum samples were centrifuged, and MMI with different concentrations was added to the supernatant.

Apparatus

An MPI-B flow injection (FI) CL analyzer (Xi'an Remex Electronic Instrument High-Tech Ltd, China) was equipped with an automatic injection system and a detection system. Polytetrafluoroethylene (PTFE) tube (0.8 mm i.d.) was used to connect all of the components in the flow system. The flow cell was a coil of glass tube that was positioned in front of the detection window of the photomultiplier tube (PMT). The static injection analysis process was measured with the static system of the MPI-B CL analyzer (Xi'an Remex Electronic Instrument High-Tech Ltd, China). In the following experiments, the voltage of PMT was 600 V. The CL spectra were obtained using a Perkin Elmer Model LS-55 luminescence spectrometer with light scours cut-off. The absorption spectra were acquired on a Thermo Nicolet Corporation Model evolution 300 UV–vis absorption spectrometer. The size and morphology of the obtained gold NPs were determined by a Hitachi 8100 transmission electron microscopy (TEM).

Experimental procedure

Preparation of gold NPs. Before synthesis of gold NPs, all glassware used was thoroughly cleaned in aqua regia (3 parts HCl, 1 part HNO_3), rinsed with Milli-Q water, and dried in an oven. Gold NPs were prepared by the Grabar's method with slight modification (27). Briefly, $HAuCl_4$ solution (0.01%, 100 mL) was boiled and trisodium citrate solution (1.0%, 2.5 mL) was added quickly with vigorous stirring. The color of the solution changed from yellow to red in a few seconds. The solution was heated for 15 min, then cooled naturally to room temperature.

FL-CL procedure. A three-channel FI-CL system was used in our experiment. One peristaltic pump (three channels) was used to carry luminol solution, H_2O and H_2O_2. Injection was performed using a six-way injection valve fitted with a 0.05 mL sample loop. The CL signal was recorded and the data were processed automatically by Remax software under Windows XP. To obtain good mechanical and thermal stability of the FI-CL system, the instruments were run for 10 min before the first measurement. Gold NPs or a mixture of gold NPs and MMI was injected into the aqueous carrier stream. The relative CL intensity ΔI ($\Delta I = I_0 - I$, where I_0 stands for the signal in the absence of MMI and I stands for the signal in the presence of MMI) showed the effect of MMI on the CL intensity of the luminol–H_2O_2–gold NPs system. It was used for quantitative analysis of MMI.

Results and discussion

Effect of MMI on the reaction of luminol–H_2O_2 catalyzed by gold NPs

The effect of MMI on the reaction of luminol–H_2O_2 catalyzed by gold NPs was investigated using the static injection analysis process. As shown in Fig. 2(a), the CL intensity of the luminol–H_2O_2 system was significantly increased in the presence of gold NPs. It was shown that the as-prepared gold NPs exhibited high catalytic activity in the luminol–H_2O_2 CL system. When MMI was introduced into gold NPs, the CL intensity of the luminol–H_2O_2 system was obviously decreased. Hence, the reaction of luminol–H_2O_2 catalyzed by gold NPs could be used to detect MMI.

Optimization of CL reaction conditions

The reaction conditions of the luminol–H_2O_2–gold NPs CL system, including reaction time of gold NPs and MMI (Fig. 2b), luminol concentration (Fig. 2c), H_2O_2 concentration (Fig. 2d), NaOH concentration (Fig. 2e), gold NP concentration (Fig. 2f) and flow rate, were carefully investigated. The binding of MMI to gold NPs results in ligand-induced aggregation of gold NPs, which had an obvious influence on the CL intensity of the luminol–H_2O_2–gold NPs system. Therefore, the effect of the reaction time of gold NPs and MMI was first considered in our CL system. As shown in Fig. 2(b), the relative CL intensity (ΔI) increased with prolonged reaction time, and reached a plateau in 20 min. Therefore, 20 min was chosen in the following experiments. Furthermore, the effects of the luminol, H_2O_2 and NaOH concentrations on the luminol–H_2O_2–gold NPs CL system were also studied. The optimized values were 6×10^{-5}, 0.1 and 0.01 mol L^{-1}, respectively. As a catalyst of the luminol–H_2O_2 CL system, gold NPs with different concentrations has an effect on the luminol–H_2O_2–gold NPs CL system. The relative CL intensity increased steadily with increasing concentration of gold NPs. Considering the CL intensity and the consumption of the gold NPs, the concentration of 1.0×10^{-5} mol L^{-1} gold NPs was used in this experiment. Finally, the effect of flow rate was also considered. The relative CL intensity markedly increased along with the increase of flow rate in the range of 1.3–4.0 mL min^{-1}. However, if the flow rate was more than 4.0 mL min^{-1}, the relative CL intensity reduced along with the increase in the flow rate. Therefore the flow rate of 4.0 mL min^{-1} was used in this experiment.

Calibration and sensitivity

Under the optimal experimental conditions, a good linear relationship (R = 0.9931) was observed up to MMI concentrations ranging from 5.0×10^{-8} to 5.0×10^{-5} mol L^{-1} and the detection limit was 1.6×10^{-8} mol L^{-1} (S/N = 3; Fig. 3). The RSD of the proposed method is 4.8% for 11 times determination of 6.0×10^{-6} mol L^{-1} MMI under the same conditions. Compared with previous reports, the proposed method has a higher sensitivity for the determination of MMI (26,28–32).

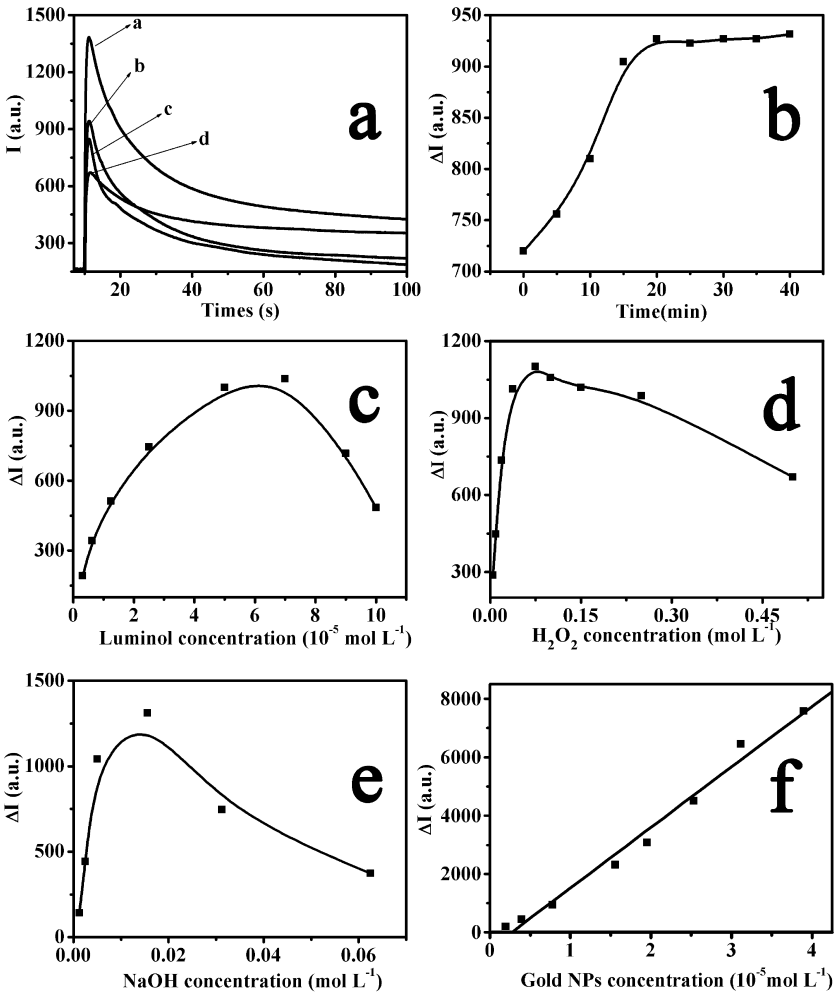

Figure 2. Effect of MMI (a), reaction time of gold NPs and MMI (b), luminol concentration (c), H_2O_2 concentration (d), NaOH concentration (e) and gold NP concentration (f) on the reaction of luminol–H_2O_2 catalyzed by gold NPs.

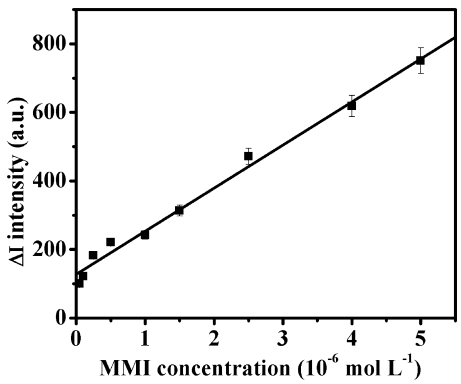

Figure 3. Linear calibration plot for methimazole. Conditions: luminol, 6.0×10^{-5} mol L^{-1}; H_2O_2, 0.1 mol L^{-1}; NaOH, 0.01 mol L^{-1}; gold NPs, 1.0×10^{-5} mol L^{-1}; flow rate, 4 mL min^{-1}; reaction time, 20 min; PMT, 600 V. Each data point was repeated five times.

Table 1. Tolerable concentration ratios with respect to 5.0×10^{-6} M MMI for some interfering species (<5% error)

Substance	Tolerance concentration ratio
Na^+, K^+, NO_3^-, NH_4^+, SO_4^{2-}	1000
Arginine, aspartic acid	100
Starch	20
Ca^{2+}, Mg^{2+}	10
Glucose	5
Cu^{2+}, Zn^{2+}, Mn^{2+}, Cr^{3+}	1

Interference studies

To evaluate the practical application of the proposed method, the influence of foreign species was studied under the same conditions by adding appropriate amounts of some foreign species to 5.0×10^{-6} mol L^{-1} MMI. A substance was considered to have no interference if the variation of the CL intensity was within ±5%. The tolerable concentration ratios of foreign species to 5.0×10^{-6} mol L^{-1} of MMI were over 1000-fold for Na^+, K^+, NO_3^-, NH_4^+ and SO_4^{2-}, 100-fold for arginine and aspartic acid, 20-fold for starch, 10-fold for Ca^{2+} and Mg^{2+}, 5-fold for glucose and 1-fold for Cu^{2+}, Zn^{2+}, Mn^{2+} and Cr^{3+} (see Table 1). It can be seen that some saline ions in the reaction system (Na^+, K^+, NO_3^-, NH_4^+, SO_4^{2-}) did not

LUMINESCENCE
The Journal of Biological and Chemical Luminescence

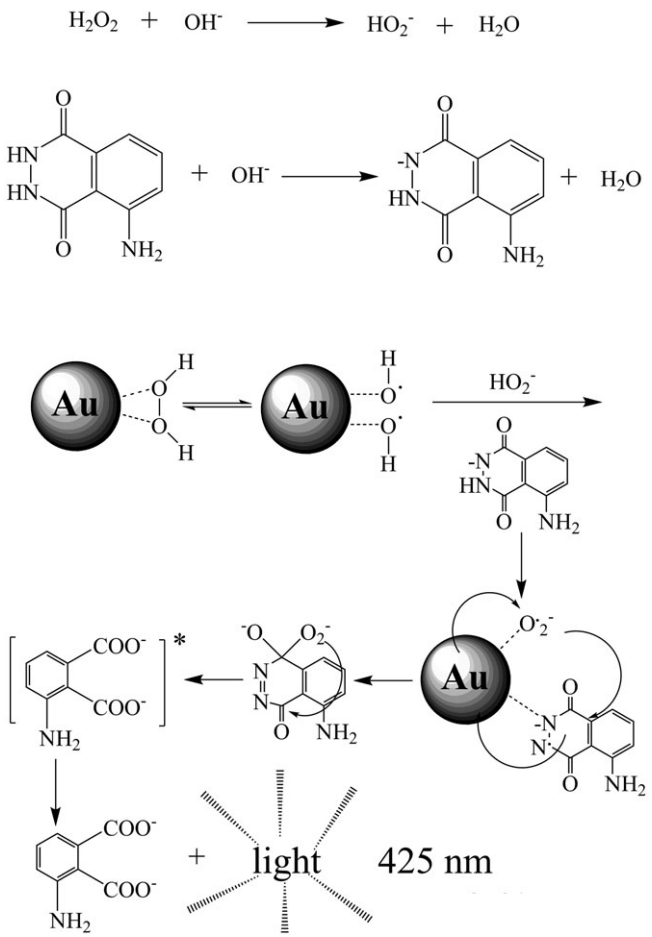

Figure 4. Scheme of a possible reaction mechanism of luminol–H_2O_2–gold NPs CL system.

affect the reaction of luminol–H_2O_2 catalyzed by gold NPs, and commonly used excipients (starch, glucose and Ca^{2+}) exhibited little influence on the determination of MMI. Therefore, the proposed method is suitable for the determination of MMI in pharmaceutical tablet.

Real sample analysis

Commercially available pharmaceutical tablets and pig serum samples were chosen to test the proposed method (Table 2). There were no significant differences between the label contents and the results obtained by the analysis of the samples. The results showed that the proposed method was suitable for analysis of pharmaceutical tablet and pig serum sample.

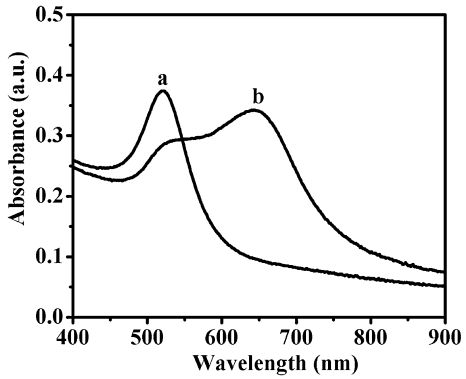

Figure 5. The UV–vis spectra of gold NPs (a) and a mixture of gold NPs and MMI (b) (gold NPs, 5.0×10^{-5} mol L^{-1}; MMI, 1.0×10^{-5} mol L^{-1}).

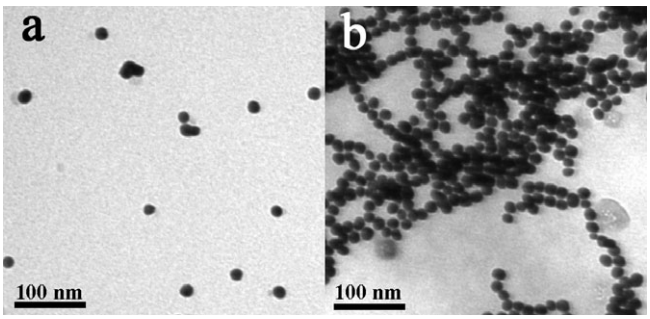

Figure 6. The TEM of gold NPs in the absence (a) and prescence of MMI (b).

Mechanism discussion

The major CL-generating mechanism of luminol–H_2O_2 catalyzed by gold NPs has been reported by Cui and co-workers (Fig. 4) (8). Gold NPs as catalyzer could break up the O–O bond of H_2O_2 that adsorbed on the surface of gold NPs into double HO radicals, which reacted with luminol anion and HO_2^- to facilitate the formation of luminol radicals. Therefore, the CL signal of the reaction of luminol and H_2O_2 increased in the presence of gold NPs.

When MMI is mixed with gold NPs, the CL intensity of luminol–H_2O_2 catalyzed by gold NPs was decreased obviously. Moreover, the wavelengths emitted in the CL reaction luminol–H_2O_2, luminol–H_2O_2–Au NPs and luminol–H_2O_2–Au NPs–MMI were 425 nm. We deduced that the possible mechanism was as follows: the binding of gold NPs to MMI resulted in aggregation of gold NPs, which reduced catalytic activity of gold NPs in the luminol–H_2O_2 CL system. To confirm our hypothesis, the UV–vis spectra and TEM of gold NPs were conducted in the presence of MMI. As shown in Fig. 5, when MMI was mixed with gold NPs, a

Table 2. Results from determination of MMI in pharmaceutical tablets (1–3) and pig serum samples (4 and 5) ($n = 5$)

Sample	Label (mg)	Found (mg)	Added (mg)	Recovered (mg)	Recovery (%)	RSD (%)
1	10.0	11.7	10.0	21.4	107.0	3.8%
2	25.0	26.1	25.0	52.1	104.0	4.1%
3	50.0	53.8	50.0	107.4	107.2	3.5%
4	0	0.2	10.0	10.8	106.0	4.6%
5	0	0.2	25.0	26.4	104.8	4.2%

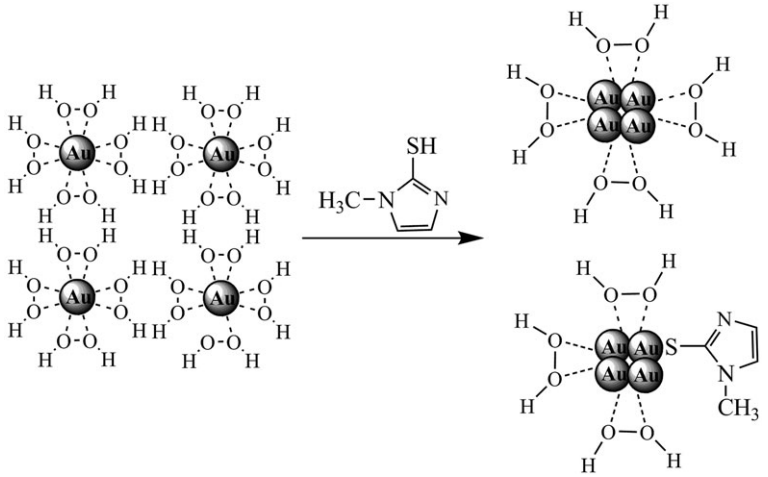

Figure 7. Scheme of a possible reaction mechanism of luminol–H_2O_2–gold NPs–MMI CL system.

new UV–vis absorption peak of gold NPs appeared at 650 nm. This indicated that conglomeration of gold NPs may have occurred. The TEM image of mixtures of gold NPs–MMI also clearly showed that gold NPs aggregate with short interparticle distance through the interaction with MMI (Fig. 6). Taking into consideration adsorption of H_2O_2 on the surface of gold NPs, we can deduce there must be competitive adsorption on the surface of gold NPs between MMI and H_2O_2, which leads to a decrease in catalytic activity of gold NPs (Fig. 7). In addition, the direct consumption of H_2O_2 by MMI may be another matter, resulting in CL inhibition. Therefore, the CL intensity of the reaction of luminol–H_2O_2 catalyzed by gold NPs was decreased in the presence of MMI.

Conclusions

A novel method for the determination of MMI was developed based on the reaction of luminol–H_2O_2 catalyzed by gold NPs. Under the optimum conditions, the detection limit was 1.6×10^{-8} mol L^{-1} (S/N = 3). Utilizing the method, the MMI content in pharmaceutical tablets and pig serum samples was determined with reasonable selectivity and sensitivity. The CL method proposed here is relatively simple and shows higher sensitivity.

Acknowledgments

The authors gratefully acknowledge the support for this research by National Natural Science Foundation of China (20675034 and 20975042), the Program for Academic Pacesetters of Wuhan (200851430484) and the Nature Science Foundation Key Project from Hubei Province of China (2008CDA080).

References

1. Ussher SJ, Yaqoob M, Achterberg EP, Nabi A, Worsfold PJ. Effect of model ligands on iron redox speciation in natural waters using flow injection with luminol chemiluminescence detection. Anal Chem 2005;77:1971–8.
2. Pavlov V, Xiao Y, Gill R, Dishon A, Kotler M, Willner I. Amplified chemiluminescence surface detection of DNA and telomerase activity using catalytic nucleic acid labels. Anal Chem 2004;76:2152–6.
3. Easton PM, Simmonds AC, Rakishev A, Egorov AM, Candeias LP. Quantitative model of the enhancement of peroxidase-induced luminol luminescence. J Am Chem Soc 1996;118:6619–24.
4. Yeha HC, Lin WY. Stopped-flow study of the enhanced chemiluminescence for the oxidation of luminol with hydrogen peroxide catalyzed by microperoxidase 8. Talanta 2003;59:1029–38.
5. Samadi-Maybodi A, Akhoondi R. Studies of visible oscillating chemiluminescence in luminol–H_2O_2–KSCN–$CuSO_4$ system using (2-hydroxyethyl) trimethylammonium hydroxide. Luminescence 2008;23:42–8.
6. Su YY, Wang J, Chen GN. Study on the enhancement of electrochemiluminescence of luminol–H_2O_2 system by sulphonated cobalt(II) phthalocyanine. Anal Chim Acta 2005;551:1–2.
7. Kuroda N, Kawazoe K, Nakano H, Wada M, Nakashima K. New phenylboronic acid derivatives as enhancers of the luminol–H_2O_2–horseradish peroxidase chemiluminescence reaction. Luminescence 1999;14:361–4.
8. Zhang ZF, Cui H, Lai CZ, Liu LJ. Gold nanoparticle-catalyzed luminol chemiluminescence and its analytical applications. Anal Chem 2005;77:3324–9.
9. Safavi A, Absalan G, Bamdad F. Effect of gold nanoparticle as a novel nanocatalyst on luminol–hydrazine chemiluminescence system and its analytical application. Anal Chim Acta 2008;610:243–8.
10. Hao E, Schatz GC, Hupp JT. Synthesis and optical properties of anisotropic metal nanoparticles. J Fluoresc 2004;14:331–41.
11. Wang ZP, Hu JQ, Jin Y, Yao X, Li JH. In situ amplified chemiluminescent detection of DNA and immunoassay of IgG using special-shaped gold nanoparticles as label. Clin Chem 2006;52:1958–61.
12. Liang SX, Li HF, Lin JM. Reaction mechanism of surfactant-sensitized chemiluminescence of bis(2,4,6-trichlorophyenyl) oxalate and hydrogen peroxide induced by gold nanoparticles. Luminescence 2008;23:381–5.
13. Zhao SL, Lan XH, Liu YM. Gold nanoparticle-enhanced capillary electrophoresis–chemiluminescence assay of trace uric acid. Electrophoresis 2009;30:2676–80.
14. Qi YY, Li BX, Zhang ZJ. Label-free and homogeneous DNA hybridization detection using gold nanoparticles-based chemiluiminescence system. Biosens Bioelectron 2009;24:3581–6.
15. Wang L, Yang P, Li YX, Chen HQ, Li MG, Luo Fb. A flow injection CL method for the determination of fluoroquinolone derivative using the reaction of luminol and hydrogen peroxide catalyzed by gold NPs. Talanta 2007;72:1066–72.
16. Li YX, Yang P, Wang P, Wang L. Development of a novel luminol chemiluminescent method catalyzed by gold nanoparticles for determination of estrogens. Anal Bioanal Chem 2007;387:585–92.
17. Li SF, Li XZ, Xu J, Wei XW. Flow-injection chemiluminescence determination of polyphenols using luminol–$NaIO_4$–gold nanoparticles system. Talanta 2008;75:32–7.
18. Wang L, Yang P, Li YX, Chen HQ, Li MG, Luo FB. A flow injection chemiluminescence method for the determination of fluoroqui-

LUMINESCENCE
The Journal of Biological and Chemical Luminescence

nolone derivative using the reaction of luminol and hydrogen peroxide catalyzed by gold nanoparticles. Talanta 2007;72:1066–72.
19. Garnera M, Armstronga DR, Reglinskia J, Smitha WE, Wilsonb R, McKillopb JH. The structure of methimazole and its consequences for current therapeutic models of graves' disease. Bioorg Med Chem Lett 1994;4:1357–60.
20. Martínez-Frías mL, Cereijo A, Rodríguez-Pinilla E, Urioste M. Methimazole in animal feed and congenital aplasia cutis. Lancet 1992;339: 742–3.
21. Wang AB, Zhang L, Zhang S, Fang YZ. Determination of thiols following their separation by CZE with amperometric detection at a carbon electrode. J Pharm Biomed 2000;23:429–36.
22. Zhang S, Sun WL, Zhang W, Qia WY, Jin LT, Yamamotob K, Tao SG, Jin JY. Determination of thiocompounds by liquid chromatography with amperometric detection at a Nafion/indium hexacyanoferrate film modified electrode. Anal Chim Acta 1999;386:21–30.
23. Zhang L, Liu Y, Xie X, Qiu YM. Simultaneous determination of thyreostatic residues in animal tissues by matrix solid-phase dispersion and gas chromatography–mass spectrometry. J Chromatogr A 2005; 1074:1–7.
24. Wasch KD, Brabander HFB, Impens S, Vandewiele M, Courtheyn D. Determination of mercaptobenzimidazol and other thyreostat residues in thyroid tissue and meat using high-performance liquid chromatography–mass spectrometry. J Chromatogr A 2001;912: 311–17.
25. Kuśmierek K, Bald E. Determination of methimazole in urine by liquid chromatography. Talanta 2007;71:2121–5.
26. Economou A, Tzanavaras PD, Notou M, Themelis DG. Determination of methimazole and carbimazole by flow-injection with chemiluminescence detection based on the inhibition of the Cu(II)-catalysed luminol–hydrogen peroxide reaction. Anal Chim Acta 2004;505:129–33.
27. Grabar KG, Freeman RG, Hommer MB, Natan MJ. Preparation and characterization of Au colloid monolayers. Anal Chem 1995;67:735–43.
28. Eshghi H, Tayyari SF, Rezvani-Amin Z, Roohi H. Methimazole-disulfide as an anti-thyroid drug metabolite catalyzed the highly regioselective conversion of epoxides to halohydrins with elemental halogens. Bull Korean Chem Soc 2008;29:51–6.
29. Sieńko D, Gugała D, Nieszporek J, Jankowska J, Saba J. Adsorption of methimazole on the mercury electrode. Electrochim Acta 2006;51: 2273–7.
30. Zakrzewski R. Determination of methimazole in urine with the iodine-azide detection system following its separation by reversed-phase high-performance liquid chromatography. J Chromatogr B 2008;869:67–74.
31. Batjoens P, Brabander HFD, Wasch KD. Rapid and high-performance analysis of thyreostatic drug residues in urine using gas chromatography–mass spectrometry. J Chromatogr A 1996;750: 127–32.
32. Aslanoglu M, Peker N. Potentiometric and voltammetric determination of methimazole. J Pharm Biomed Anal 2003;33:1143–7.

